Observed Properties of Exoplanets: Masses, Orbits, and Metallicities

Geoffrey MARCY,[1,*] R. Paul BUTLER,[2] Debra FISCHER,[3]
Steven VOGT,[4] Jason T. WRIGHT,[1] Chris G. TINNEY[5] and Hugh R. A. JONES[6]

[1]*Astronomy Department, University of California, Berkeley, CA 94720, USA*
[2]*Department of Terrestrial Magnetism, Carnegie Institution of Washington, 5241 Broad Branch Rd NW, Washington DC 20015-1305, USA*
[3]*Department of Physics and Astronomy, San Francisco State University, San Francisco, CA 94132, USA*
[4]*UCO/Lick Observatory, University of California at Santa Cruz, Santa Cruz, CA 95064, USA*
[5]*Anglo-Australian Observatory, PO Box 296, Epping 1710, Australia*
[6]*Centre for Astrophysics Research, University of Hertfordshire, Hatfield, AL10 9AB, UK*

We review the observed properties of exoplanets found by the Doppler technique that has revealed 152 planets to date. We focus on the ongoing 18-year survey of 1330 FGKM type stars at Lick, Keck, and the Anglo-Australian Telescopes that offers both uniform Doppler precision (3 m s^{-1}) and long duration. The 104 planets detected in this survey have minimum masses ($M \sin i$) as low as 6 $M_{\rm Earth}$, orbiting between 0.02 and 6 AU. The core-accretion model of planet formation is supported by four observations: 1) The mass distribution rises toward the lowest detectable masses, $dN/dM \propto M^{-1.0}$. 2) Stellar metallicity correlates strongly with the presence of planets. 3) One planet (1.3 $M_{\rm Sat}$) has a massive rocky core, $M_{\rm Core} \approx 70\ M_{\rm Earth}$. 4) A super-Earth of $\sim 7\ M_{\rm Earth}$ has been discovered. The distribution of semi-major axes rises from 0.3 – 3.0 AU ($dN/d\log a$) and extrapolation suggests that ∼12% of the FGK stars harbor gas-giant exoplanets within 20 AU. The median orbital eccentricity is $\langle e \rangle = 0.25$, and even planets beyond 3 AU reside in eccentric orbits, suggesting that the circular orbits in our Solar System are unusual. The occurrence "hot Jupiters" within 0.1 AU of FGK stars is 1.2±0.2%. Among stars with one planet, 14% have at least one additional planet, occasionally locked in resonances. Kepler and COROT will measure the occurrence of earth-sized planets. The Space Interferometry Mission (SIM) will detect planets with masses as low as 3 $M_{\rm Earth}$ orbiting within 2 AU of stars within 10 pc, and it will measure masses, orbits, and multiplicity. The candidate rocky planets will be amenable to follow-up spectroscopy by the "Terrestrial Planet Finder" and Darwin.

§1. Introduction

In the past 10 years, 152 exoplanets have been discovered orbiting 131 normal stars by using the Doppler technique to monitor the gravitational wobble induced by a planet, as previously summarized.[56),59)] Multiple planet systems have been detected around 17 of the 131 planet-bearing stars, found by superimposed multiple Doppler periodicities.[59),83)] Remarkable statistical properties have emerged from the 152 planets:

- Planet mass distribution: $dN/dM \propto M^{-1.0}$ (Fig. 1)

*) E-mail: gmarcy@berkeley.edu

- >7% of stars have giant planets within 5 AU, most beyond 1 AU (Fig. 2)
- Hot Jupiters ($a < 0.1$ AU) exist around 1.2% of FGK stars
- Eccentric Orbits are common, with a median of $\langle e \rangle = 0.25$ (Fig. 3)
- Planet occurrence rises rapidly with stellar metallicity (Fig. 6)
- Multiple planets are common, often in resonant orbits (Fig. 7)

Four planets of extraordinarily low mass have been found. Three have Neptune-like masses of $M \sin i$ of 21, 15, and 18 $M_{\rm Earth}$ orbiting host stars, GJ 436, 55 Cancri, and HD 190360, respectively.[12),60),83)] The fourth planet is likely the first "super-Earth" with $M \sin i = 6.0$ $M_{\rm Earth}$ and $P = 1.94$ d, orbiting the star, GJ 876.[68)] Apparently, planet formation can populate the mass range between that of Uranus and Earth.

The first direct image of an exoplanet has finally occurred with the VLT/NACO and HST/NICMOS images of 2M1207 and its companion separated by 773 mas (54 AU projected separation).[17),71)] At the likely age (8 Myr) of this system in the TW Hydrae association, the IR photometry implies a mass of 2–5 $M_{\rm Jup}$ based on atmospheric models of such young, warm planets.[6),11)] The second epoch HST observations (Schneider, private communication) confirm that the companion is bound to the primary, rendering it the first planetary mass companion ever imaged.

To date, 7 planets are known that cross the disk of their star, 5 found photometrically by the dimming of the star.[3),9),79)] However, the two closest stars with transiting planets (HD 209458, HD 149026) were found first by the Doppler method.[13),34),70)] The fractional dimming of the star's flux gives a direct measure of the radius of the planet relative to the stellar radius that is determined from stellar modelling. The edge-on orbit and Doppler measurements give the planet mass. The resulting densities of these planets are in the range of 0.2–1.4 g/cm^3 verifying the expectation that the planets are gaseous (albeit with *liquid* metallic hydrogen interiors).[13),34)] During transit, starlight passing through the planet's atmosphere has allowed detection of its constituents, notably sodium and hydrogen.[14),82)] During eclipse of the planet by the star, measurements of the diminished infrared flux in narrow bands permit assessment of the atmospheric temperature and other atmospheric constituents such as water vapor and methane.[15),19)] From precise Doppler measurements, including the Rossiter effect (in which the planet blocks a portion of the rotating star's hemisphere, causing a net Doppler shift), the tidal heating has been shown to be negligible, leaving the large radius of HD 209458 unexplained.[49),87)] Most remarkable is HD 149026 that has only 1.21 $M_{\rm Sat}$ but a high density of 1.4 g/cm^3 (twice Saturn's), implying the existence of a massive rocky core of 70 $M_{\rm Earth}$.[70)]

The standard theory for the formation of gas giant planets is the "core-accretion" model that begins with dust particles colliding and growing within a protoplanetary disk to form rock-ice planetary cores.[1),30),33),39),42)–44),51),53),86)] If the core becomes massive enough while gas remains in the disk, it gravitationally accretes nearby gas, acquiring an extended gaseous envelope.[7),8),61),65)] Support for the core-accretion model has come from HD 149026b with its massive rocky core and implied high abundance of heavy elements, suggesting that core formation dominated any acquisition

of gas, as discussed by Sato et al. (2005).

Gas giants accrete most of the gas within their tidal reach filling the Hill sphere around them with the heated, gaseous envelope. Further gas accretion is slowed both by the diminishing amounts of remaining local gas and by the extended envelope, leading to predicted growth times of 5–10 Myr. This growth time scale is uncomfortably longer than the observed ∼3 Myr lifetime of the disks themselves.[31),32)] Therefore the original core accretion model suffers from a planet-growth rate that is too slow.

This inadequacy in the core-accretion model has been addressed in two ways. Inward migration of type I[52),75),76),85)] will bring giant planets to fresh, gas-rich regions of the disk.[2),4)] Moreover, improved opacities are lower, allowing more rapid escape of radiation that speeds the shrinkage of the envelope to accelerate the accretion of more gas. The resulting planet growth time scale is shortened to ∼1 Myr, well within the lifetime of protoplanetary disks.[2),4),35),36)]

Giant planets probably form preferentially *beyond 3 AU* where their tidal reach permits accretion of large amounts of cool disk gas. In contrast, we find that 1.2% of stars harbor giant planets *within 0.1 AU*, suggesting that the planets migrated inward. Strong evidence of migration comes from the numerous resonances among the multi-planet systems that suggests migrational settling into the resonance traps.[16),45),48),50),67),83)] Migration may occur by two primary processes. Planets may lose energy and angular momentum to the disk (type I) causing inward migration, or the disk gas may viscously accrete onto the star, dragging planets with them (type II)[10),16),18),37),52),80),85)]

The origin of the orbital eccentricities remains poorly understood, as interactions between planet and gaseous disk are thought to damp eccentricities.[5),76),84)] If so, *the orbital eccentricities must arise after the major stage of gas accretion.* Subsequent gravitational interactions among planets and between planets and the disk may cause the observed orbital eccentricities, perhaps related to resonant interactions between planets.[10),16),23),26),28),36),48),50),58),62),67),77)]

The properties of the masses and orbits of observed giant planets are becoming well represented by the current models[2),45)] including the correlation of planets with metallicity[37)] and with stellar mass[38)] (see Ida & Lin in this issue).

§2. The Lick, Keck, and the Anglo-Australian planet search

The determination of the statistical properties of giant planets depends on a survey of planets that has well-understood detection thresholds in both mass and orbital period. We have carried out precise radial velocity measurements of 1330 FGKM dwarfs at the Lick, Keck 1, and Anglo-Australian telescopes. The majority of stars had their first high-quality measurement between 1995 and 1998, giving a time coverage of ∼7–10 years thus far. The target stars and their properties are available,[81),88)] and were drawn from the Hipparcos catalog[20)] with criteria that they have $B - V > 0.55$, reside no more than 3 mag above the main sequence (to avoid photospheric jitter seen in giants), and have no stellar companion within 2 arcsec (to avoid confusion at the entrance slit).

The target list also includes 120 M dwarfs, located mostly within 10 pc with declination north of -30 deg.[88] For the late-type K and M dwarfs, we restricted our selection to stars brighter than $V = 11$. All slowly rotating stars are surveyed with a Doppler precision of 3 m s^{-1} to provide a uniform sensitivity to planets. Thus far, our Lick, Keck, and Anglo-Australian surveys have revealed 104 planets orbiting 88 stars, including 12 multi-planet systems. The orbital elements and masses of these exoplanets are regularly updated at: `http://exoplanets.org` .

§3. Observed properties of exoplanets

We derive the statistical properties of planets from the 1330 FGKM target stars for which we have uniform precision of 3 m s^{-1} and at least 6 years duration of observations. Detected exoplanets have minimum masses, $M \sin i$, between 6 $M_{\rm Earth}$ and $\sim$15 $M_{\rm Jup}$, with an upper mass limit corresponding to the (vanishing) tail of the mass distribution. The planet mass distribution is shown in Fig. 1 and follows a power law, $dN/dM \propto M^{-1.05}$ [54),55)] affected very little by the unknown $\sin i$.[41] The paucity of companions with $M \sin i$ greater than 12 $M_{\rm Jup}$ confirms the presence of a "brown dwarf desert"[54] for companions with orbital periods up to a decade.

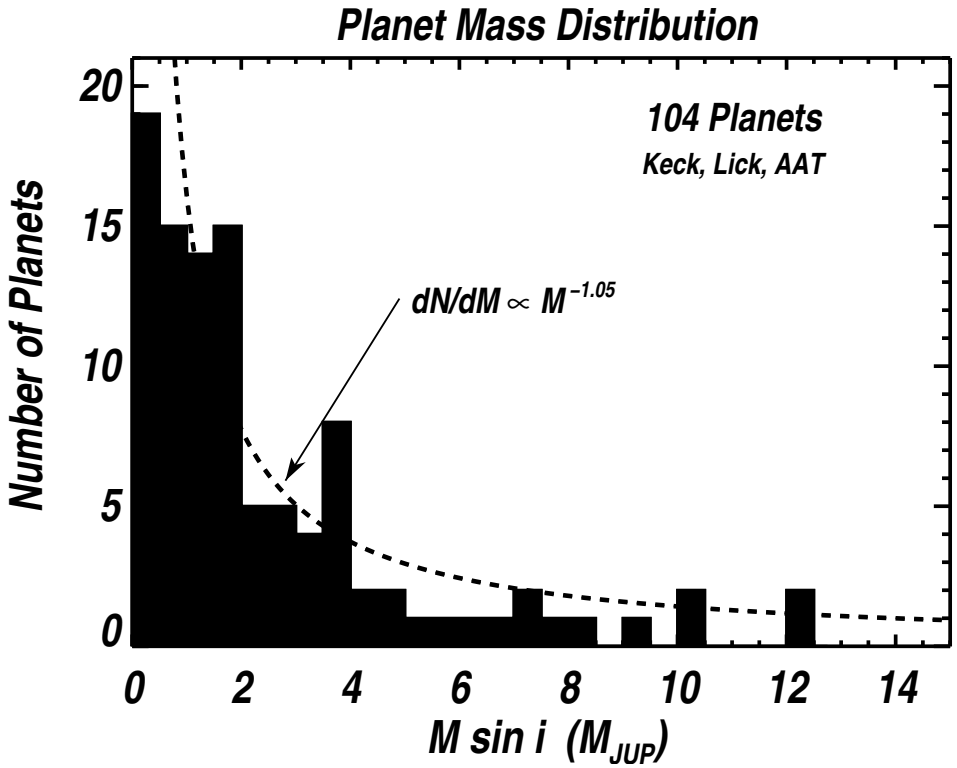

Fig. 1. The histogram of 104 planet masses ($M \sin i$) found in the uniform 3 m s^{-1} Doppler survey of 1330 stars at Lick, Keck, and the AAT telescopes. The bin size is 0.5 $M_{\rm Jup}$. The distribution of planet masses rises as $M^{-1.05}$ from 10 $M_{\rm Jup}$ down to Saturn masses, with incompleteness at lower masses.

The 88 stars with planets among the 1330 target stars imply that the fraction of stars harboring giant planets with $M < 13 M_{\rm Jup}$ within 5 AU is at least 88/1330 = 6.6%. This is no doubt a lower limit as planets between 3–5 AU are not efficiently detected due to the limited duration, 6–8 years, of our Doppler survey. The 12 stars with two or more planets imply an occurrence rate of at least 1% for systems with multiple giant planets.

The observed semimajor axes span the range 0.02–6.0 AU. We have found 16 planets that orbit within 0.1 AU, implying that such "hot" Jupiters exist around 16/1330 = 1.2±0.3% of FGK main sequence stars.[40),56)] The number of planets increases with distance from the star from 0.3 to 3 AU, as shown in Fig. 2 (in logarithmic bins). A modest (flat) extrapolation suggests that a comparable population of yet-undetected jupiters exists between 5–20 AU, bringing the occurrence of giant planets to roughly 12% within 20 AU (Fig. 2). Indeed, some 5% of our stars show a long term trend in velocity, suggestive of a planetary companion between 5 and 20 AU.

The orbital eccentricities for the 104 detected exoplanets are plotted versus semi-

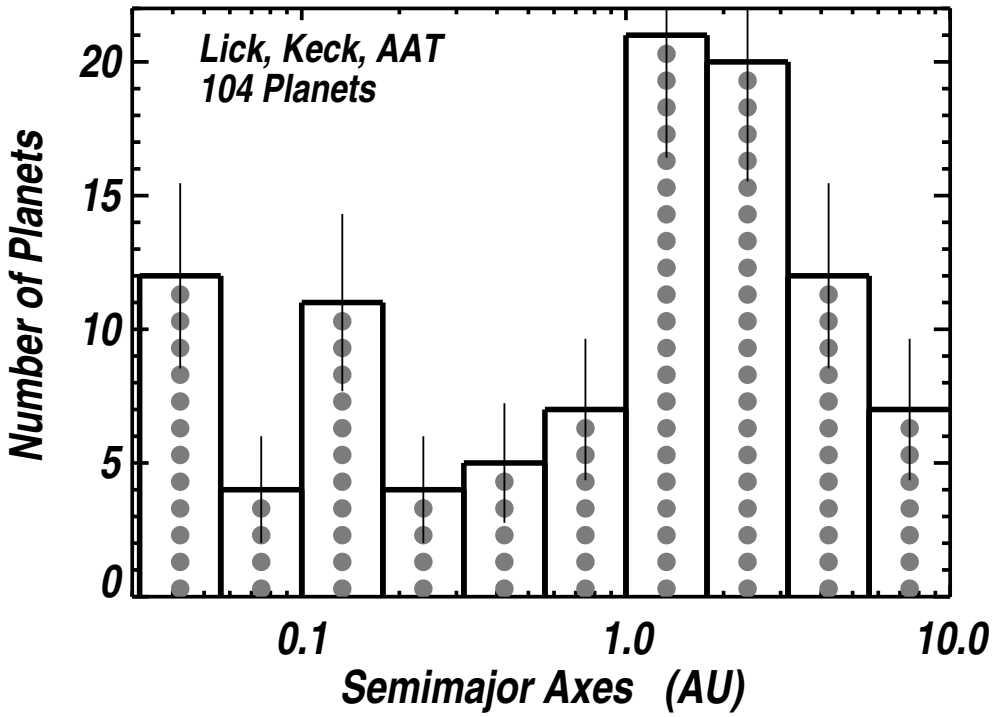

Fig. 2. Histogram of semimajor axes, a, of the 104 exoplanets found from the Doppler survey at Lick, Keck, and the AAT Telescopes. Note the equal logarithmic bins, $\Delta \log a$. There are increasing numbers of planets toward larger orbits beyond 0.5 AU. The occurrence of planets within 3 AU is 6.6%. There is increasing incompleteness beyond 3 AU. Flat extrapolation from 3–20 AU suggests that ∼12% of all nearby FGK stars have a giant planet with mass greater than Saturn.

major axis in Fig. 3. Apparently eccentricities span the full available range, 0.0–1.0, but avoiding those with such small periastron distances, $r_{\rm min} = a(1-e)$ <0.1, that tidal circularization would occur. Indeed, planets orbiting within 0.1 AU are all in nearly circular orbits, presumably due to tidal circularization.

However, planets orbiting beyond 0.1 AU (i.e. not circularized) have a median eccentricity of $\langle e \rangle = 0.25$ with a standard deviation of 0.19. Thus, the orbital eccentricities of giant planets within 5 AU are considerably higher than those in our Solar System. Remarkably, among the planets farthest from the host star, a = 2–4 AU, there is no tendency for them to have small eccentricities. The indications from our velocity data suggest that exoplanets having $a \approx 5.2$ AU will also have non-zero eccentricities. It may be years before we are able to distinguish definitively true eccentricities at 5 AU from multiple planets. In the upcoming years we expect to discover a population of exoplanets at $a \approx 5.2$ AU that will allow direct comparison of cosmic eccentricities with that of Jupiter, $e = 0.048$.

Our 104 planets can be examined for any relationship between planet mass and semimajor axis. We plot planet mass vs semimajor axis for our 104 planets in Fig. 4. The upper left region of the plot is devoid of planets, indicating that massive planets

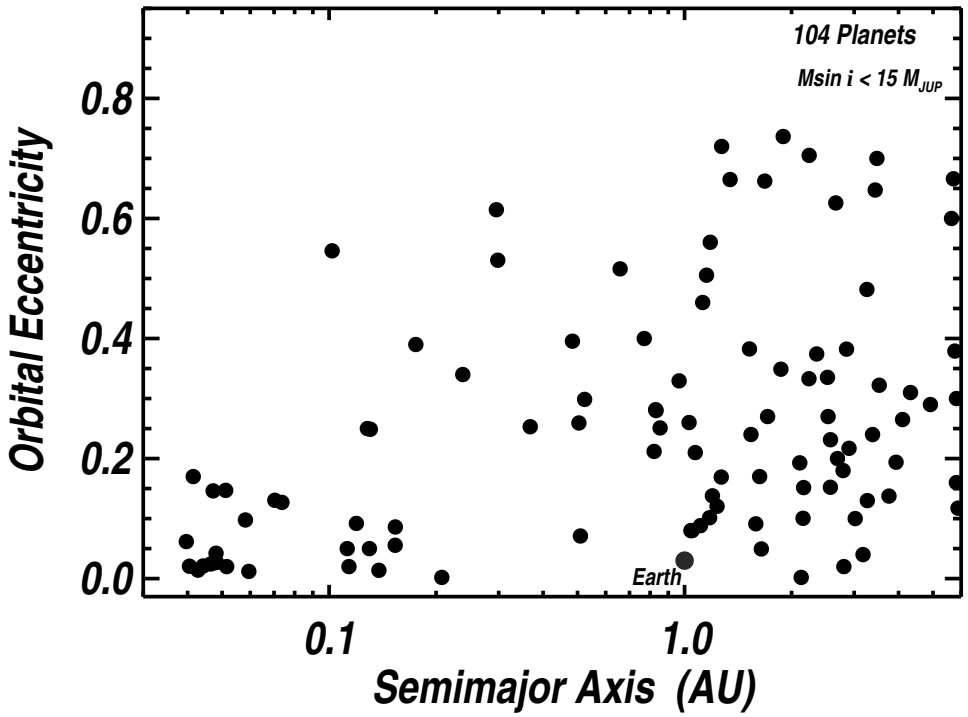

Fig. 3. Eccentricity vs semimajor axis, for the 104 planets discovered in the Lick, Keck, and AAT Doppler survey. Eccentricity ranges from 0 to 0.8 and no decline in eccentricity is observed beyond 3 AU. It seems quite likely that giant planets at 5.2 AU also reside in eccentric orbits, in contrast to Jupiter in our Solar System.

rarely are found close to the host star. Our Doppler survey, with its uniform Doppler precision of 3 m s^{-1} and duration of ∼8 years would have easily found massive planets orbiting within 1 AU of target stars. Thus, this paucity of massive, close-in planets is not a selection effect and is statistically real.[89)]

However, we might ask if the mass distribution for planets orbiting beyond 1 AU is actually different from those within 1 AU. Interestingly, the planets both beyond and within 1 AU have a mass distribution that increases toward lower masses (Fig. 4). The small number of high mass planets within 1 AU may be simply due to the small total number of planets orbiting close in. With our precision of 3 m s^{-1}, planets beyond 1 AU having low masses are certainly missed, both because they induce a small wobble and because few orbits have transpired during our program. Thus while the small number of massive planets orbiting close to host stars is real, there is no strong evidence that the mass distribution is a function of orbital distance.

We may also consider the dependence of orbital eccentricity on planet mass. In Fig. 5, we plot eccentricity vs $M \sin i$ for the 104 planets found in our Doppler survey, but we include only those 86 planets orbiting with a >0.1 AU, to avoid those that may have been tidally circularized. Figure 5 shows no strong correlation between

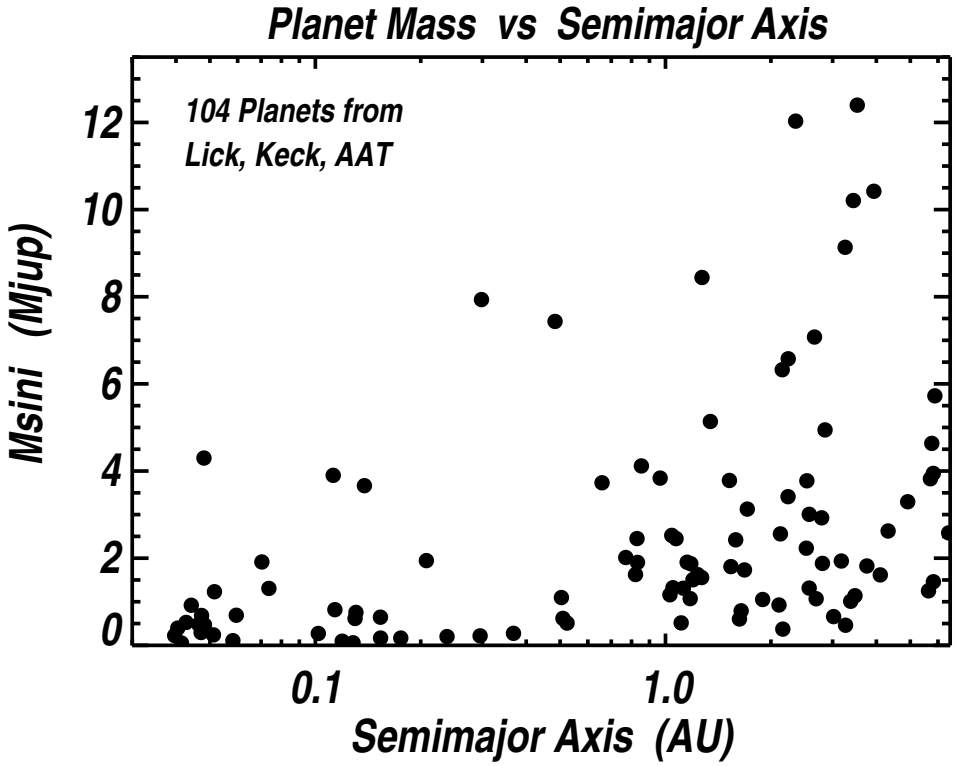

Fig. 4. Planet mass vs semimajor axis for the 104 planets found at Lick, Keck, and the AAT. There is a dearth of close-in planets having high mass that cannot be a selection effect as our survey would surely discover the massive, close-in planets. However, the distribution of masses for close-in planets may be similar to that for planets *beyond* 1 AU, considering the difficulty in detecting low mass planets beyond 1 AU.

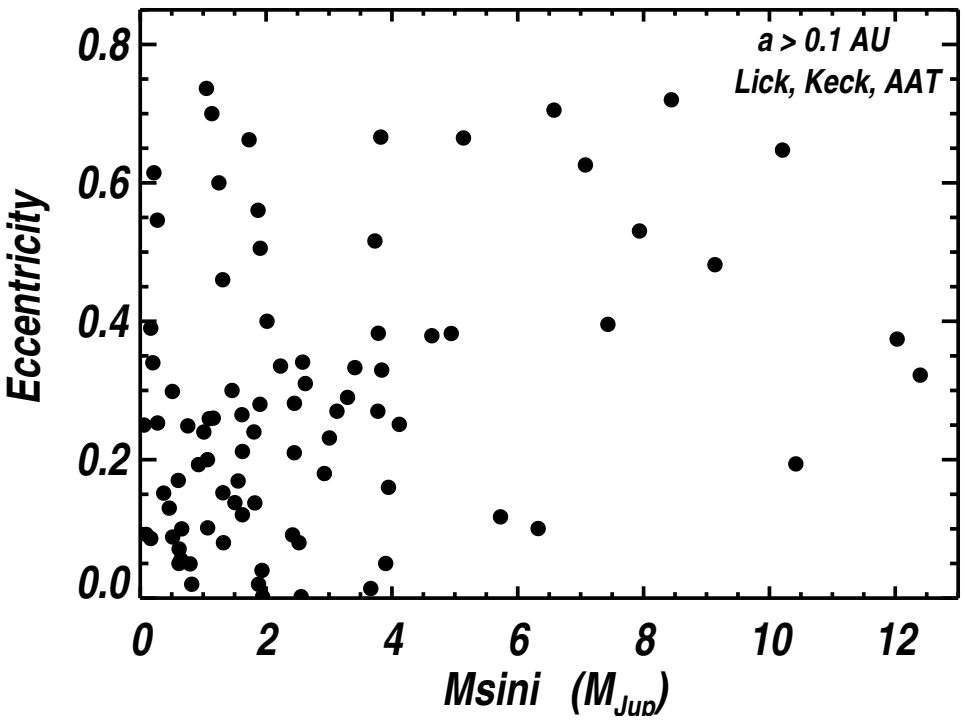

Fig. 5. Orbital eccentricity vs Planet mass ($M \sin i$) for the 104 planets found in our survey. A strong correlation is not seen. However, planets of highest mass tend to have higher orbital eccentricities than those of lower mass. This is puzzling, as higher mass planets require greater perturbations to alter orbits that were originally circular.

eccentricity and planet mass. However, the most massive planets, notably those with $M \sin i > 5\, M_{\rm Jup}$, exhibit systematically higher eccentricities than do the planets of lower mass. This cannot be a selection effect nor can it be caused by errors because the most massive planets (right half) induce the largest Keplerian amplitudes, K, allowing accurate determination of eccentricity.

If planets form initially in circular orbits, the high eccentricities of the most massive planets in Fig. 5 poses a puzzle. Such massive planets have the greatest inertial resistance to perturbations that are necessary to drive them out of their initial circular orbits. Yet the massive planets reside mostly in orbits more eccentric than the lower mass planets. We remain puzzled that the most massive planets have the highest orbital eccentricities. *Perhaps massive planets formed by a process in which the orbits are not initially circular.*

3.1. *Planet-metallicity correlation*

Planet occurrence correlates strongly with the abundance of heavy elements in the host star, as shown in Fig. 6. In our survey of FGK stars, ∼25% of the most metal-rich stars, [Fe/H] $> +0.3$, harbor planets while fewer than 3% of the metal poor stars, [Fe/H] < -0.5 have detected planets.[21),29),66),69)]

A power-law fit to the occurrence of planets as a function of [Fe/H] yields

$$\mathcal{P}(\text{planet}) = 0.03 \times \left(\frac{(\text{N}_{\text{Fe}}/\text{N}_{\text{H}})}{(\text{N}_{\text{Fe}}/\text{N}_{\text{H}})_{\odot}} \right)^2 .$$

Apparently the occurrence of gas giant planets is nearly proportional to the square of the number of iron atoms. This is consistent with collision rates, suggesting that the dust particle growth rate in the protoplanetary disk is related to the final existence of a gas giant planet. This steep dependence of planet occurrence on metallicity lends weight to the core accretion model.

The physical mechanism for the observed planet-metallicity correlation is often cast as "nature or nurture". In the former case, high metallicity enhances planet formation because of increased availability of small particle condensates, the building blocks of planetesimals.[46] In the latter case, enhanced stellar metallicity is due to the late-stage accretion of gas-depleted, dust-rich material, causing "pollution" of the star's convective zone (CZ). These two mechanisms leave different and distinguishable marks on the host stars. In the former case, the star is metal-rich throughout its interior. In the latter case, additional metals are mixed from the photosphere only throughout the convective zone, leaving the interior of the star with lower metallicity.

There is strong support for the former "nature" hypothesis. Of particular importance, the metallicities of stars are independent of both CZ depth and of evolution across the subgiant branch (where dilution is expected due to a deepening CZ). While accretion of metals must occur for all pre-main-sequence stars, the stars with extrasolar planets appear to have enhanced metals extending below the CZ. Thus it is unlikely that the high metallicity of planet-bearing stars is caused by accretion. Furthermore, planet-bearing stars with super-solar metallicity are more than twice as likely to have multiple planet systems than planet-bearing stars with sub-solar metallicity. Taken together, these findings suggest that initial high metallicity enhances planet formation, providing support for the core accretion model of giant planet formation.

§4. Multi-planet systems and the lowest mass planets

Among 152 exoplanets found by all Doppler teams, 131 stars harbor a single planet, 14 stars have two known planets, two have three known planets (Upsilon And and HD 37124), and one has four detected planets (55 Cancri). Thus, multi-planet systems exist in 17 of 131 (13%) of known planet-bearing stars. This fraction is certainly a lower limit, as multiple systems demand more Doppler observations to extract the multiple signals. The 17 known multi-planet systems are shown in Fig. 7, with each planet shown at its semimajor axis and with a dot diameter proportional to $M \sin i$.

There is preference for the lower mass planet to reside inward of the outer planets. Such an effect is expected if the disk accretion onto the inner planets is blocked by accretion onto the outer planet.[45] However this modest mass difference between inner and outer planets could also be a selection effect. Outer planets that are lower

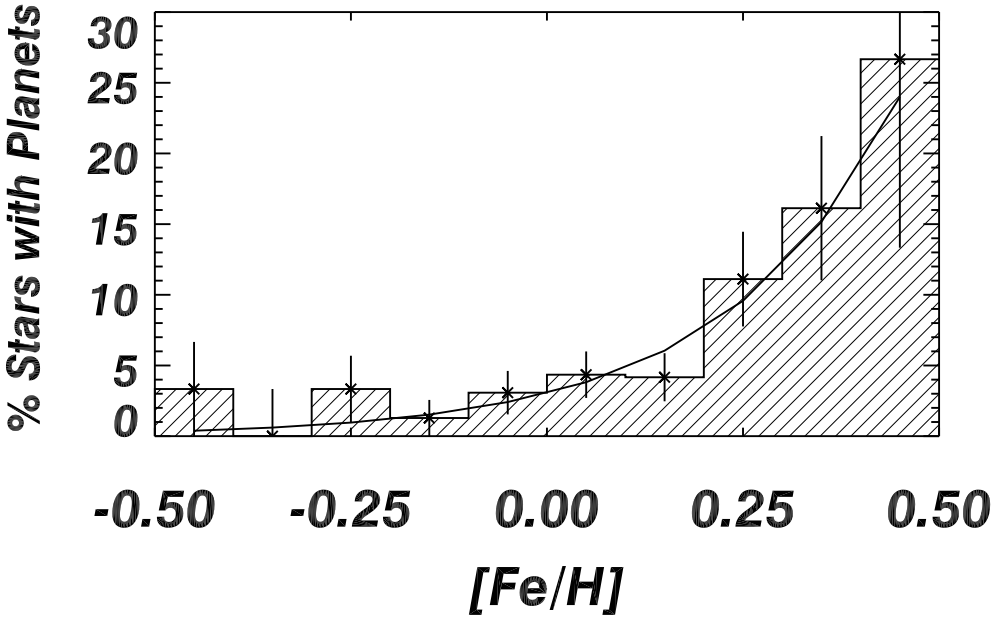

Fig. 6. The occurrence of exoplanets vs iron abundance [Fe/H] of the host star measured spectroscopically.[21] The occurrence of observed giant planets increases strongly with stellar metallicity. The solid line is a power law fit for the probability that a star has a detected planet: $\mathcal{P}(\text{planet}) = 0.03 \times 10^{2.0 \times [\text{Fe/H}]}$

mass can be absorbed in the model of a single, more massive planet located closer to the host star. Additional planets continue to emerge in the set of stars with known planets as more observations are obtained and as Doppler precision improves.

We have found three "Neptune-class" planets with minimum masses of 21, 15, and 18, $M_{\rm Earth}$, all with short periods of 2.5–10 d around host stars, GJ 436, 55 Cancri, and HD 190360, respectively.[12),60),83)] We have also found the first "super-Earth", with $M \sin i = 6.0\ M_{\rm Earth}$. Its orbital period is $P = 1.94$ d around the star GJ 876, joining its two resonant Jupiter-mass planets. Apparently, planets exist that are intermediate in mass between the ice giants and the terrestrial planets. Such planets may form in dusty disks that have little gas.

The Doppler method with state-of-the-art precision of 1 m s^{-1} can reveal planets having masses as low as 10 $M_{\rm Earth}$ for periods less than 5 d. But astrophysical noise ("jitter") caused by stellar surface turbulence, spots, and stellar acoustic p-modes make the detection of planets below 10 $M_{\rm Earth}$ difficult, notably due to the unpredictable, stochastic interference of the acoustic p-modes in Solar-type stars.

The Doppler detection of Earth-mass planets orbiting a Solar-mass star at $\sim$1 AU will require a 6-meter class, dedicated telescope to detect the Doppler amplitude of only $\sim$0.1 m s^{-1}. An alternative approach will be to search for low-mass planets by achieving 1 m s^{-1} precision for much lower-mass stars. Surveys of M- and L-dwarfs with masses 0.1 $M_\odot$ at 1 m s^{-1} would also allow the the detection of sub-10 $M_{\rm earth}$ planets, though such searches will require the use of either much larger telescopes in

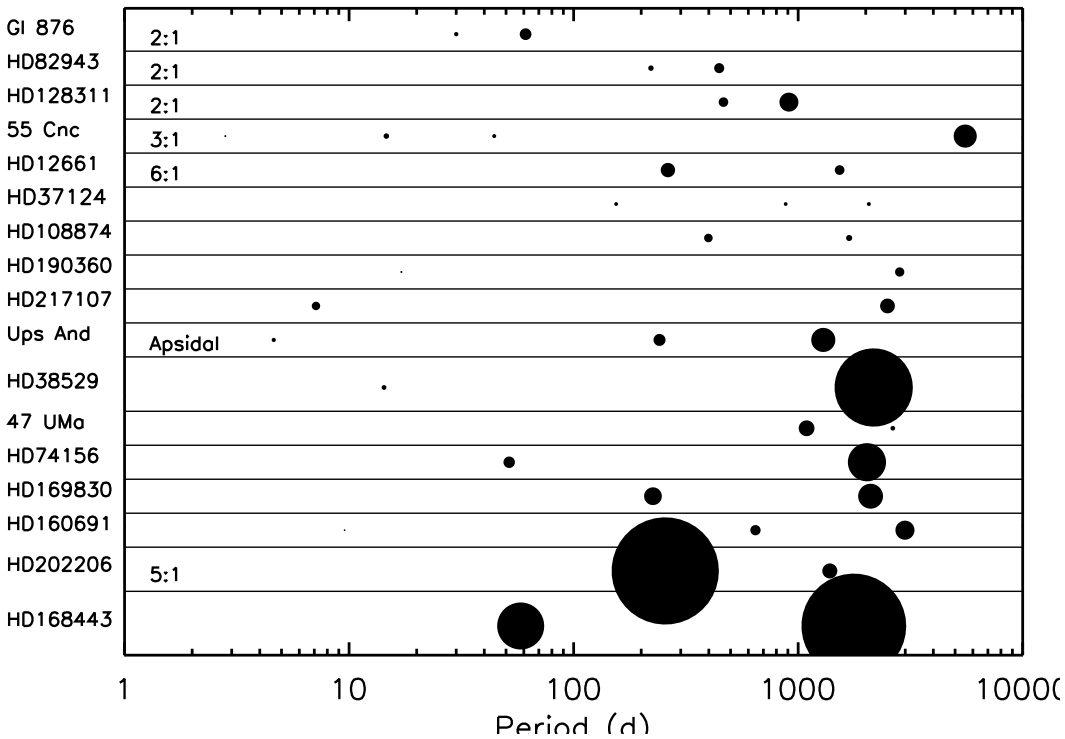

Fig. 7. The known 17 multi-planet systems. The dots mark the orbital period of each planet and the diameter of each dot is proportional to $M \sin i$. There is a modest tendency for the inner planets of multi-planet systems to be the least massive, interpretable either as suppressed accretion from the outer disk, or as a mere selection effect.

the optical (where these stars are very faint), or a new generation of near-infrared echelle spectrographs on 8m-class telescopes.

The Kepler and COROT missions are designed to photometrically detect Earth-mass planets during transits of the host star, providing the first measure of the occurrence of rocky planets and ice-giants. However, the host stars will reside at typical distances beyond 250 pc, making imaging and spectroscopic follow-up of the planets difficult. A method is needed to detect earth-mass planets around nearby stars, amenable to follow-up.

§5. The Space Interferometry Mission

The Space Interferometry Mission, SIM, will do astrometry by using a 9-meter baseline and optical wavelengths to measure the optical path delay. The precision for stars brighter than $V = 10$ will be 1.5 μas. SIM will carry out Galactic and extragalactic projects that require high astrometric precision, 1.5–20 μas, during its nominal five-year mission starting in 2011. SIM will carry out a search for rocky planets around $\sim$250 stars located within 20 pc.

The technical specifications of SIM are provided by 72). SIM will be carried into

an Earth-trailing solar orbit via an expendable launch vehicle and will slowly drift away from the Earth at 0.1 AU/yr, reaching 0.6 AU after 5.5 years. It will obtain fringes at a set of wavelengths from 400–900 nm, from which optical path delays will be measured. The 9 meter baseline vector between the two mirrors is established by a separate guide interferometer that monitors bright stars.

The astrometry of each target star is carried out relative to at least 3 reference stars located within ∼1 deg. Ideally, the three reference stars should spatially encompass the target star to constrain the differential angular separations in both of two axes. Ideally, the reference stars are bright ($V < 10$) and distant (∼1 kpc) giants so that the astrometric "noise" due to planets around them is minimized. Candidate reference stars having brown dwarf or stellar companions within 10 AU are identified and rejected by using repeated (and ongoing) radial velocity measurements that we acquire from ground-based telescopes at a precision of 20 m s^{-1} .[27] At $V = 10$ mag, a ten-chop sequence between target and each reference star, with 30 sec integrations per chop, will achieve the 1.5 μas precision, including instrumental and photon-limited errors. Spots on the youngest, most active, stars will move their photocenters by $\sim 1\mu$as, but stars older than 2 Gyr have spot covering factors less than 0.2%, making the spots insignificant.

5.1. *Finding earth-mass planets with SIM*

The SIM search for rocky planets around nearby stars includes ∼250 AFGKM-type targets within 20 pc. Several criteria governed the selection of target stars, including proximity and large angular separation of their habitable zones. The highest priority members of the target list are listed at
`http://www.physics.sfsu.edu/SIM/`

SIM will detect planets with masses greater than 3 $M_{\rm Earth}$ orbiting between 0.1 and 2 AU around nearby stars. It will determine the masses, orbits, and multiplicity of planets, and will permit correlation of these properties with the star's mass and metallicity. Rocky planets detected by SIM will be separated from the host star by ∼0.3 arcsec, offering opportunities for surgical follow-up observations by existing ground-based and space-borne telescopes. Thus, SIM is expected to initiate an era of characterization of rocky planets. Moreover, the SIM results provide reconnaissance for later imaging missions such as TPF and Darwin.

5.2. *The lowest mass planets detectable by SIM*

The detection thresholds by SIM have been assessed by 24), 73) and 74) with special attention paid to secure detections of rocky planets. Here, we consider the detectability by SIM of planets having the lowest detectable masses of 3 $M_{\rm Earth}$ and below.

We simulate SIM measurements of a planet in a circular orbit at 1 AU orbiting a star of 0.7 $M_\odot$ at 5 pc, typical of stars on the SIM target list and the nearest stars on the TPF target lists. We adopt an assumed inclination of $i = 60$ deg which acts to suppress the astrometric signal in one dimension. We consider two cases of 30 and 50 SIM observations (in each of two dimensions) obtained during 5 years with expected astrometric errors of 1.5 μas.

The timing of the simulated observations was semi-random with a minimum separation in observations of 30 days because the lowest mass planets cannot be detected in short periods. In any case, detection efficiency is not a sensitive function of the cadence of observations.[24] We imposed gaps in the observing sequence to account for the 4 month sun-avoidance time which introduces detection blind spots near periods of 1.0 and 0.5 years. The current key planet-search projects have been allocated sufficient time for 24 observations in both dimensions of ∼135 stars. However, allocation of additional observing time is being requested and adaptive scheduling algorithms may allow observations to be timed to optimize detections after early data are acquired.[26]

Detection of 3 $M_{\rm Earth}$ planets around such stars is challenging because the astrometric wobble of 2.5 μas is only slightly larger than SIM errors, 1.5 μas. However, the points carry a temporal coherence with orbital phase, making a detection possible. One detection approach is to fit the data with a Keplerian model to obtain χ^2 and determine the associated False Alarm Probability (FAP) by using Keplerian fits to mock velocity sets that contain no planet.

Here, we simplify the estimate of FAP by computing a periodogram of the astrometric measurements along both axes (labelled "RA" and "DEC") and determining the FAP by Monte Carlo of data sets that have no planet. Figure 8 shows (at left) a

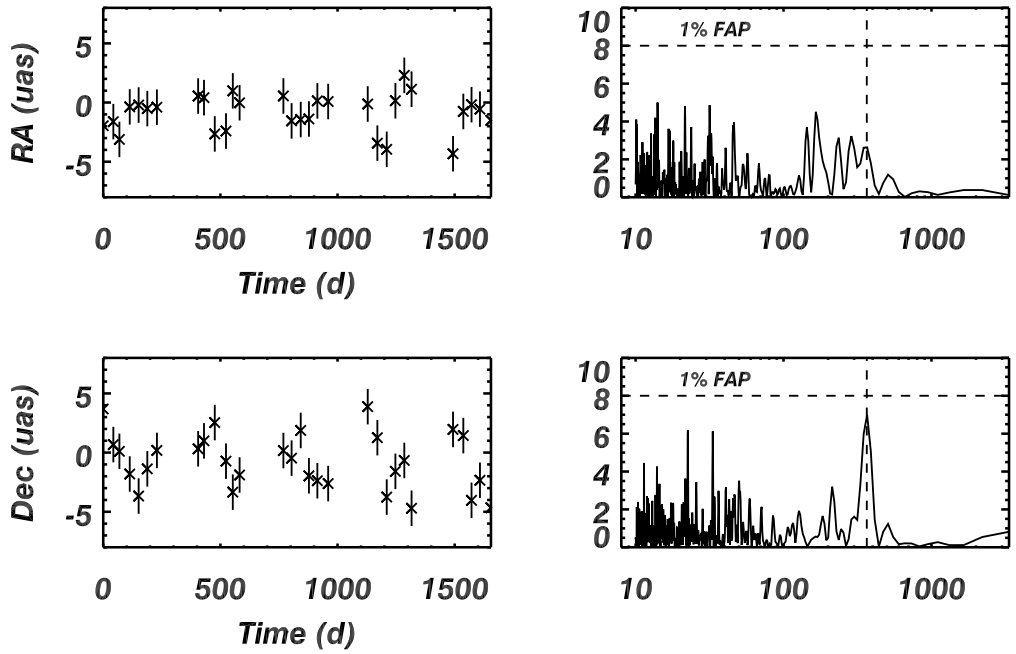

Fig. 8. Simulation of 30 SIM measurements in orthogonal directions (labeled RA and DEC) for a 3 $M_{\rm Earth}$ planet orbiting at 1 AU from a 0.7 $M_\odot$ star at 5 pc. The periodicity in the DEC measurements (long axis) is marginally apparent. The periodogram of position for the RA and DEC measurements is shown at right. For the DEC measurements, the signal has a FAP of just above 1%, implying that planets of 3 $M_{\rm Earth}$ at 1 AU are marginally detectable (star at 5 pc).

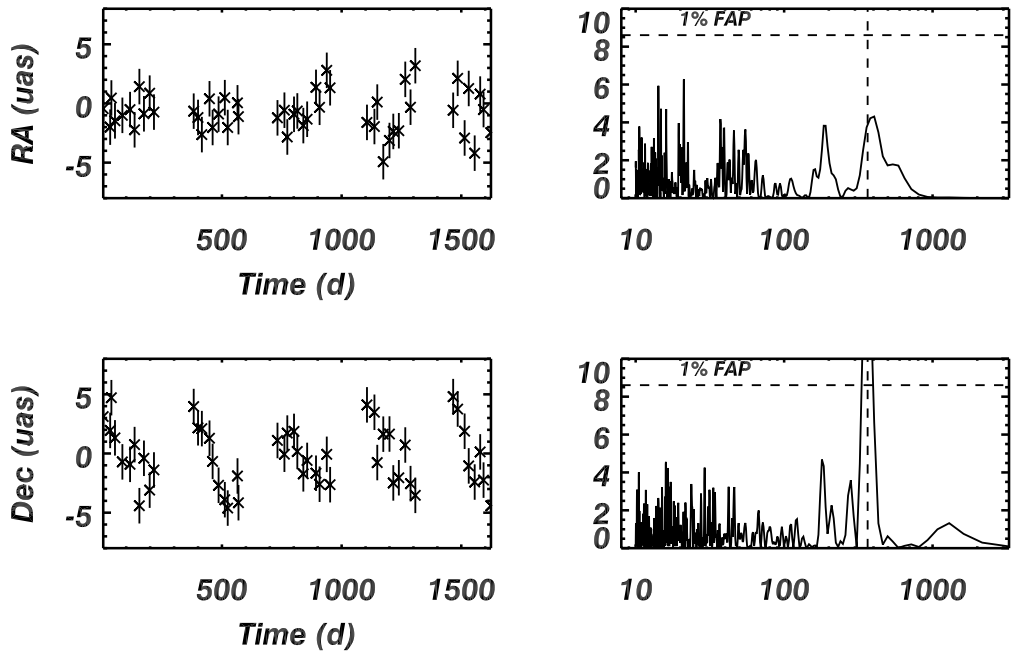

Fig. 9. Same as Fig. 8, but for 50 observations. The 3 $M_{\rm Earth}$ stands out strongly in the periodogram, due to the extra observations.

typical set of simulated astrometric measurements (due to the 3 $M_{\rm Earth}$ planet and 1.5 μas noise) in both RA and DEC, the latter showing a marginal periodicity to the eye (the arbitrary inclination suppresses the signal in RA). At right in Fig. 8, the periodogram of the astrometric measurements shows a peak residing just below the 1% FAP threshold. *Thus, with only 30 observations SIM can just detect planets of 3 $M_{\rm Earth}$ orbiting at 1 AU around Solar type stars at 5 pc.*

If 50 SIM observations are made, the astrometric periodicity in the signal stands out strongly, as shown in Fig. 9. Thus, there is a steep improvement in the detectability of planets of 3 $M_{\rm Earth}$ by increasing the number of observations from 30 to 50, due to signal being comparable to the errors. These results are similar to those of Sozzetti et al.[73] who assumed somewhat fewer observations per star.

We have run 1000 realizations of the two cases, 30 and 50 observations for this same case of a 3 $M_{\rm Earth}$ planet orbiting at 1 AU around 0.7 $M_{\odot}$ star at 5 pc. The cumulative distribution function of FAP values from the trials is shown in Fig. 10. The distribution shows that with 50 observations, planets of 3 $M_{\rm Earth}$ are easily detected and carry low FAP, typically below 0.01. However, if only 30 observations are made, the FAP is typically 0.04 or above in order for 80% of these planets are to be detected. Even with only 30 observations, SIM is capable of detecting planets of 3 $M_{\rm Earth}$ with 63% efficiency, incurring a FAP of only $\sim$2%. SIM can also identify stars highly likely to harbor planets of slightly lower mass, but with successively higher FAP.

We also considered a 1.5 $M_{\rm Earth}$ planet orbiting (as before) with $P \approx 1$ yr around

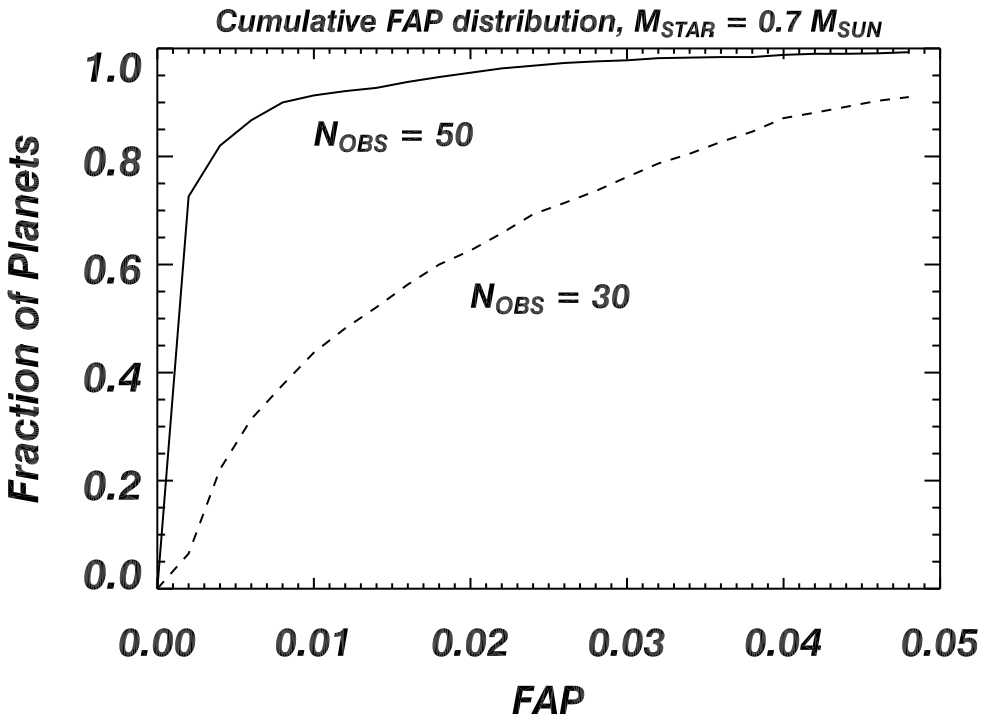

Fig. 10. The fraction of 3 $M_{\rm Earth}$ planets in the Habitable Zone that are detectable by SIM, as a function of the associated False Alarm Probability (FAP) for two cases: 30 and 50 SIM observations. The simulations adopt the nominal SIM astrometric precision of 1.5 μas in each orthogonal direction, and adopt random times of observation, excluding sun-avoidance times. The host star is assumed to have mass of 0.7 $M_{\odot}$, at a distance of 5 pc, representative of nearby late G and K dwarfs. For the case of 50 observations, 98% of planets having 3 $M_{\rm Earth}$ are detected, for an adopted FAP in the signal of 0.03 (3% of stars will incur a false detection of a planet). For 30 observations, 75% of the 3 $M_{\rm Earth}$ planets will be detected at FAP = 0.03. Thus, SIM will detect the majority of 3 $M_{\rm Earth}$ planets and incur modest false alarms.

a 0.7 $M_{\odot}$ star at 5 pc. For this lower mass planet, the astrometric wobble is slightly less than the measurement errors of 1.5 μas, making detection even more challenging. However, Monte Carlo trials of such a system typically yield a weak but apparent periodogram peak corresponding to FAP = 3–5% with only 30 measurements, as shown in Fig. 11. *Thus, SIM can marginally detect planets of 1.5 $M_{\rm Earth}$ orbiting at ∼1 AU around Solar type stars at 5 pc, albeit with considerable false alarms.* Nonetheless these marginal detections will provide a subsample of stars that are enriched in planets of 1.5–3.0 $M_{\rm Earth}$, useful for follow-up work.

§6. The synergy of SIM and TPF/Darwin

The simulations of SIM observations of Earth-mass planets show that 3 $M_{\rm Earth}$ planets are detectable and 1.5 $M_{\rm Earth}$ planets are marginally found at 5 pc. Thus, the SIM survey of 200 nearby stars will identify a subset that has planets of 3–10

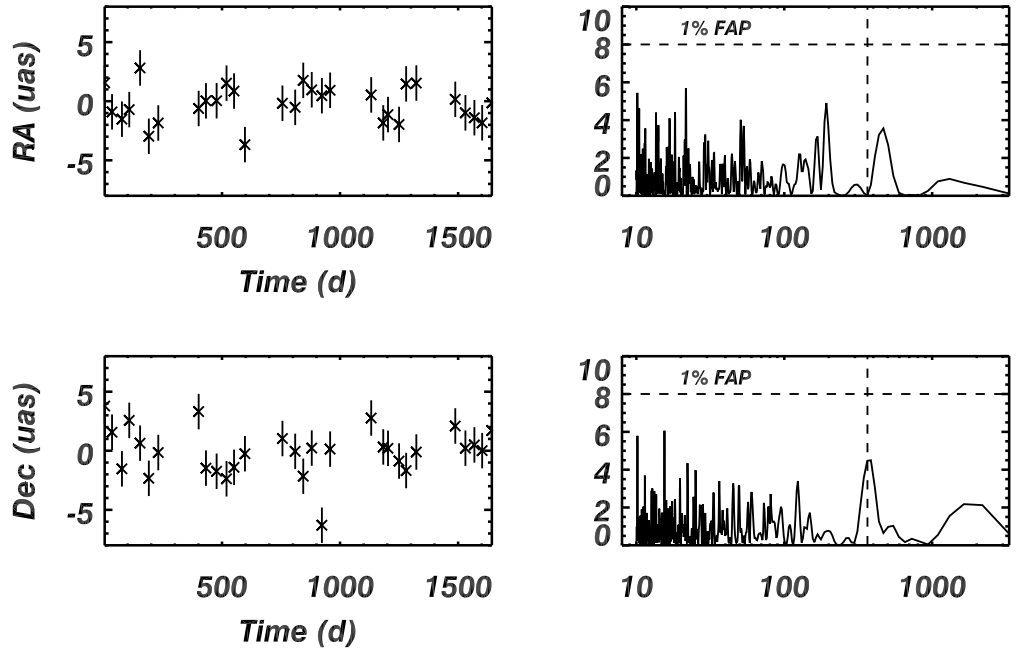

Fig. 11. Simulated 30 SIM measurements in orthogonal directions for a 1.5 $M_{\rm Earth}$ planet orbiting with $P \approx 1$ yr from a 0.7 $M_{\odot}$ star. The periodicity in the DEC measurements (long axis) is apparent weakly in the periodogram for the DEC measurements at the correct period of $P =$ 365 d, but with a FAP of 4%, typical of the 100 trials. Thus, planets of 1.5 $M_{\rm Earth}$ at 1 AU are only marginally detectable.

$M_{\rm Earth}$ (should they be common) and another subset that is likely to have even lower mass planets, 1.5–3.0 $M_{\rm Earth}$, albeit with some false alarm interlopers. SIM can thus produce an input sample of nearby stars that is enriched by about a factor of 3 in 1.5–3 $M_{\rm Earth}$ planets over an original sample. Assuming, for example, that the fraction of stars with earths in the habitable zone, $\eta_{\rm Earth}$, is 0.1, it is easy to show that SIM will produce an output list of stars that is enriched by a factor of 3 in habitable earths over the original input sample of stars. Thus, SIM will provide TPF and Darwin with target stars having either strong or plausible evidence of rocky planets. SIM will also identify those stars that TPF and Darwin should avoid, notably those with a large planet near the habitable zone that renders any earths dynamically unstable. Of course, any such saturn or neptune-mass planets within 2 AU will be valuable themselves for planetary astrophysics.

If $\eta_{\rm Earth}$ is indeed ∼10%, TPF/Darwin will be hard pressed to detect these few earths because of their rarity and their faintness, $V \approx 30$ mag. Moreover, for modestly inclined orbital planes, TPF/Darwin will miss planets located angularly within the diffraction-limited "inner working angle" (IWA $= \sim 4\lambda/D = 0.065$ arcsec for TPF-C). A planet orbiting 1 AU from a star located 5 pc away will spend roughly 1/3 of its orbit inside the IWA, leaving it undetected. *Thus if the occurrence of earths in habitable zones is of order 10%, SIM will triple the efficiency of TPF and Darwin*

both by identifying the likely host stars and by predicting the orbital phase during which the earth is farthest from the glare of the host star.

SIM alone provides a wealth of planetary astrophysics, including the masses, orbital radii, and orbital eccentricities of rocky planets around the nearest stars. It will also find correlations between rocky planets and stellar properties such as metallicity and rotation. With a lifetime extended beyond 5 years, SIM can detect planets of even lower mass, down to 1 $M_{\rm Earth}$.

SIM and TPF/Darwin together, along with Kepler, provide a valuable combination of information about rocky planets. Kepler offers the occurrence rate of small planets. SIM provides the masses and orbits of planets around nearby stars, identifying the candidate earths. TPF/Darwin measure radii, chemical composition, and atmospheres. In some cases, images from TPF/Darwin may feedback on the analysis of old SIM data, helping orbit determination especially for multiple planetary systems.

Acknowledgements

We thank John Johnson, Chris McCarthy, Brad Carter, and Alan Penny for their work on the Doppler planet search. We thank the SIM Project team at JPL, especially Michael Shao, Chas Beichman, Steven Unwin, Shri Kulkarni, Chris Gelino, Joe Catanzerite and Jo Pitesky. We appreciate support by NASA grant NAG5-75005 and NSF grant AST-0307493.

References

1) S. J. Aarseth, D. N. C. Lin and P. L. Palmer, Astrophys. J. **403** (1993), 351.
2) Y. Alibert, C. Mordesini, W. Benz and C. Winisdoerffer, Astron. Astrophys. **434** (2005), 343.
3) R. Alonso et al., Astrophys. J. **613** (2004), L153.
4) P. J. Armitage, C. J. Clarke and F. Palla, Mon. Not. R. Astron. Soc. **342** (2003), 1139.
5) P. Artymowicz, Astrophys. J. **419** (1993), 166.
6) I. Baraffe, G. Chabrier, F. Allard and P. H. Hauschildt, Astron. Astrophys. **382** (2002), 563.
7) P. Bodenheimer and J. B. Pollack, Icarus **67** (1986), 391.
8) P. Bodenheimer, G. Laughlin and D. N. C. Lin, Astrophys. J. **592** (2003), 555.
9) F. Bouchy, C. Melo, N. C. Santos, M. Mayor, D. Queloz and S. Udry, Astron. Astrophys. **431** (2005), 1105.
10) G. Bryden, M. Różyczka, D. N. C. Lin and P. Bodenheimer, Astrophys. J. **540** (2000), 1091.
11) A. Burrows et al., Astrophys. J. **491** (1997), 856.
12) R. P. Butler, S. S. Vogt, G. W. Marcy, D. A. Fischer, J. T. Wright, G. W. Henry, G. Laughlin and J. J. Lissauer, Astrophys. J. **617** (2004), 580.
13) D. Charbonneau, T. M. Brown, D. W. Latham and M. Mayor, Astrophys. J. **529** (2000), L45.
14) D. Charbonneau, T. M. Brown, R. Noyes and R. Gilliland, Astrophys. J. **568** (2001), 377.
15) D. Charbonneau, L. E. Allen, S. T. Megeath, G. Torres, R. Alonso, T. M. Brown, R. L. Gilliland, D. W. Latham, G. Mandushev, F. T. O'Donovan and A. Sozzetti, Astrophys. J. **626** (2005), 523.
16) E. I. Chiang and N. Murray, Astrophys. J. **576** (2002), 473.
17) G. Chauvin, A.-M. Lagrange, C. Dumas, B. Zuckerman, D. Mouillet, I. Song, J.-L. Beuzit and P. Lowrance, Astron. Astrophys. **425** (2004), L29.
18) G. D'Angelo, W. Kley and T. Henning, Astrophys. J. **586** (2003), 540.

19) D. Deming, S. Seager, L. J. Richardson and J. Harrington, Nature **434** (2005), 740.
20) ESA (1997), VizieR Online Data Catalog, 1239, 0.
21) D. A. Fischer and J. A. Valenti, Astrophys. J. **622** (2005), 1102.
22) E. B. Ford and S. Tremaine, Publ. Astron. Soc. Pac. **115** (2003), 1171.
23) E. B. Ford, F. A. Rasio and K. Yu, ASP Conf. Ser. **294** (2003), 181.
24) E. B. Ford, Publ. Astron. Soc. Pac. **116** (2004), 1083.
25) E. B. Ford, Astron. J. (2005), submitted.
26) E. B. Ford, V. Lystad and F. Rasio, Nature (2005), submitted.
27) S. Frink, A. Quirrenbach, D. A. Fischer, S. Röser and E. Schilbach, Publ. Astron. Soc. Pac. **113** (2001), 173.
28) K. Goździewski, Astron. Astrophys. **398** (2003), 315.
29) G. Gonzalez, Mon. Not. R. Astron. Soc. **285** (1997), 403.
30) R. Greenberg, W. K. Hartmann, C. R. Chapman and J. F. Wacker, Icarus **35** (1978), 1.
31) K. E. Haisch, E. A. Lada and C. J. Lada, Astrophys. J. **553** (2001), L153.
32) L. Hartmann, N. Calvet, E. Gullbring and P. D'Alessio, Astrophys. J. **495** (1998), 385.
33) C. Hayashi, Prog. Theor. Phys. Suppl. No. 70 (1981), 35.
34) G. W. Henry, G. W. Marcy, R. P. Butler and S. S. Vogt, Astrophys. J. **529** (2000), L41.
35) O. Hubickyj, P. Bodenheimer and J. J. Lissauer, Revista Mexicana de Astronomia y Astrofisica Conference Series **22** (2004), 83.
36) S. Ida and D. N. C. Lin, Astrophys. J. **604** (2004), 388. (2004b)
37) S. Ida and D. N. C. Lin, Astrophys. J. **616** (2004), 567. (2004b)
38) S. Ida and D. N. C. Lin, Astrophys. J., "Towards a deterministic model of planetary formation. III. Mass distribution of short-period planets around stars of various masses", (2005), in press.
39) M. Ikoma, K. Nakazawa and E. Emori, Astrophys. J. **537** (2000), 1013.
40) H. R. A. Jones, R. P. Butler, C. G. Tinney, G. W. Marcy, C. McCarthy, A. J. Penny and B. D. Carter, ASP Conf. Ser. **321** (2004), 298.
41) A. Jorissen, M. Mayor and S. Udry, Astron. Astrophys. **379** (2001), 992.
42) E. Kokubo and S. Ida, Icarus **131** (1998), 171.
43) E. Kokubo and S. Ida, Icarus **143** (2000), 15.
44) E. Kokubo and S. Ida, Astrophys. J. **581** (2002), 666.
45) W. Kley, M.-H. Lee, N. Murray and S. Peale, Astrophys. J. (2005), in press.
46) K. Kornet, P. Bodenheimer, M. Różyczka and T. F. Stepinski, Astron. Astrophys. **430** (2005), 1133.
47) M. Konacki, G. Torres, D. D. Sasselov and S. Jha, Astrophys. J. **597** (2003), 1076.
48) G. Laughlin and J. E. Chambers, Astrophys. J. **551** (2001), L109.
49) G. Laughlin, G. W. Marcy, S. S. Vogt, D. A. Fischer and R. P. Butler, Astrophys. J. (2005), in press, "On the Eccentricity of HD 209458".
50) M. H. Lee and S. J. Peale, Astrophys. J. **567** (2002), 596.
51) H. F. Levison, J. J. Lissauer and M. J. Duncan, Astron. J. **116** (1998), 1998.
52) D. N. C. Lin, J. C. B. Papaloizou, C. Terquem, G. Bryden and S. Ida, Protostars and Planets IV (2000), 1111.
53) J. J. Lissauer, Icarus **114** (1995), 217.
54) G. W. Marcy and R. P. Butler, Publ. Astron. Soc. Pac. **112** (2000), 137.
55) G. W. Marcy, R. P. Butler, D. A. Fischer and S. S. Vogt, ASP Conf. Ser. **294** (2003), 1.
56) G. W. Marcy, R. P. Butler, D. A. Fischer and S. S. Vogt, ASP Conf. Ser. **321** (2004), 3. (2004b)
57) G. W. Marcy, R. P. Butler, S. S. Vogt, D. A. Fischer, G. W. Henry, G. Laughlin, J. T. Wright and J. Johnson, Astrophys. J. **619** (2005), 570.
58) F. Marzari and S. J. Weidenschilling, Icarus **156** (2002), 570.
59) M. Mayor, S. Udry, D. Naef, F. Pepe, D. Queloz, N. C. Santos and M. Burnet, Astron. Astrophys. **415** (2004), 391.
60) B. McArthur, M. Endl, W. D. Cochran, G. F. Benedict, D. A. Fischer, G. W. Marcy and R. P. Butler, Astrophys. J. **614** (2004), 81.
61) H. Mizuno, Prog. Theor. Phys. Suppl. No. 64 (1980), 54.
62) R. P. Nelson and J. C. B. Papaloizou, Mon. Not. R. Astron. Soc. **333** (2002), L26.
63) M. Podolak, Icarus **165** (2003), 428.
64) M. Podolak, Revista Mexicana de Astronomia y Astrofisica Conference Series **22** (2004),

104.
65) J. B. Pollack et al., Icarus **124** (1996), 62.
66) I. N. Reid, Publ. Astron. Soc. Pac. **114** (2002), 306.
67) E. J. Rivera and J. J. Lissauer, Astrophys. J. **558** (2001), 392.
68) E. J. Rivera, J. J. Lissauer, R. P. Butler, G. W. Marcy, S. S. Vogt, D. A. Fischer, T. M. Brown, G. Laughlin and G. W. Henry, Astrophys. J. (2005), in press.
69) N. C. Santos, G. Israelian and M. Mayor, Astron. Astrophys. **415** (2004), 1153.
70) B. Sato, D. A. Fischer, G. W. Henry, G. Laughlin, R. P. Butler, G. W. Marcy, S. S. Vogt, P. Bodenheimer, A. Wolf, M. Ammons, L. Boyd, S. Ida, J. A. Johnson, C. McCarthy, D. Minnniti, S. Robinson, J. Strader, K. L. Tah, E. Toyota, J. Valenti and J. T. Wright, submitted to Astrophys. J.
71) G. Schneider et al., American Astronomical Society Meeting Abstracts (2004), 205,
72) M. Shao, *Interferometry in Space*, ed. Michael Shao, Proceedings of the SPIE **4852** (2003).
73) A. Sozzetti, S. Casertano, R. A. Brown and M. G. Lattanzi, Publ. Astron. Soc. Pac. **114** (2002), 1173.
74) A. Sozzetti, S. Casertano, R. A. Brown and M. G. Lattanzi, Publ. Astron. Soc. Pac. **115** (2003), 1072.
75) H. Tanaka, T. Takeuchi and W. R. Ward, Astrophys. J. **565** (2002), 1257.
76) H. Tanaka and W. R. Ward, Astrophys. J. **602** (2004), 388.
77) E. W. Thommes and J. J. Lissauer, Astrophys. J. **597** (2003), 566.
78) G. Torres, M. Konacki, D. D. Sasselov and S. Jha, American Astronomical Society Meeting **203** (2003).
79) G. Torres, M. Konacki, D. D. Sasselov and S. Jha, Astrohpys. J. **619** (2005), 558.
80) D. E. Trilling, J. I. Lunine and W. Benz, Astron. Astrophys. **394** (2002), 241.
81) J. A. Valenti and D. A. Fischer, Astrophys. J. (2005), in press.
82) A. Vidal-Madjar, J.-M. Desert, A. Lecavelier des Etangs, G. Hebrard, G. Ballester, D. Ehrenreich, R. Ferlet, J. McConnell, M. Mayor and C. Parkingson, Astrophys. J. **604** (2004), L69.
83) S. S. Vogt, R. P. Butler, G. W. Marcy, D. A. Fischer, G. W. Henry, G. Laughlin, J. T. Wright and J. Johnson, Astrophys. J. (2005), in press.
84) W. R. Ward, Icarus **106** (1993), 274.
85) W. R. Ward, Astrophys. J. **482** (1997), L211.
86) G. W. Wetherill and G. R. Stewart, Icarus **77** (1989), 330.
87) J. Winn, R. W. Noyes, G. W. Marcy, R. P. Butler et al., Astrophys. J. (2005), in prep., "Measurement of spin-Orbit Alignment in an Extrasolar Planetary System".
88) J. T. Wright, G. W. Marcy, R. P. Butler and S. S. Vogt, Astrophys. J. Suppl. **152** (2004), 261.
89) S. Zucker and T. Mazeh, ASP Conf. Ser. **294** (2003), 31.